Lepton flavor violating radion decays in the Randall-Sundrum scenario

E. O. Iltan, *B. Korutlu †
Physics Department, Middle East Technical University
Ankara, Turkey

Abstract

We predict the branching ratios of the lepton flavor violating radion decays $r \to e^\pm \mu^\pm$, $r \to e^\pm \tau^\pm$ and $r \to \mu^\pm \tau^\pm$ in the two Higgs doublet model, in the framework of the Randall-Sundrum scenario. We observe that their branching ratios are at most of the order of 10^{-8}, for the small values of radion mass and they decrease with the increasing values of m_r. Among these processes, the $r \to \tau^\pm \mu^\pm$ decay would be the most suitable one to measure its branching ratio.

*E-mail address: eiltan@newton.physics.metu.edu.tr
†E-mail address: beste.korutlu@gmail.com

1 Introduction

The hierarchy problem between weak and Planck scales could be explained by introducing the extra dimensions. One of the possibility is to pull down the Planck scale to TeV range by considering the compactified extra dimensions of large size [1]. The assumption that the extra dimensions are at the order of submilimeter distance, for two extra dimensions, the hierarchy problem in the fundamental scales could be solved and the true scale of quantum gravity would be no more the Planck scale but it is of the order of electroweak (EW) scale. This is the case that the gravity spreads over all the volume including the extra dimensions, however, the matter fields are restricted in four dimensions, so called four dimensional (4D) brane. Another possibility, which is based on the non-factorizable geometry, is introduced by Randall and Sundrum [2] (the RS1 model) and, in this scenario, the extra dimension is compactified to S^1/Z_2 orbifold with two 4D brane boundaries. Here, the gravity is localized in one of the boundary, so called the Planck (hidden) brane, which is away from another boundary, the TeV (visible) brane where we live. The size of extra dimension is related to the vacuum expectation of a scalar field and its fluctuation over the expectation value is called the radion field (see section 2 for details). The radion in the RS1 model has been studied in several works in the literature [3]-[13] (see [14] for extensive discussion).

In the present work, we study the possible lepton flavor violating (LFV) decays of the radion field r. The LFV interactions exist at least in one loop level in the extended standard model (SM), so called νSM, which is constructed by taking neutrinos massive and by permitting the lepton mixing mechanism [15]. Their negligibly small branching ratios (BRs) stimulate one to go beyond and they are worthwhile to examine since they open a window to test new models and to ensure considerable information about the restrictions of the free parameters, with the help of the possible accurate measurements. The LFV interactions are carried by the flavor changing neutral currents (FCNCs) and in the SM with extended Higgs sector (the multi Higgs doublet model) they can exist at tree level. Among multi Higgs doublet models, the two Higgs doublet model (2HDM) is a candidate for the lepton flavor violation. In this model, the lepton flavor violation is driven by the new scalar Higgs bosons S, scalar h^0 and pseudo scalar A^0, and it is controlled by the Yukawa couplings appearing in lepton-lepton-S vertices.

Here, we predict the BRs of the LFV r decays in the 2HDM, in the framework of the RS1 scenario [1]. The BRs of these processes are sensitive to the new Yukawa couplings arising with

[1] The flavor conserving decays of the radion can exist in the tree level and the theoretical values of the BRs are free from the loop suppressions. For the heavy flavor output $\tau\tau$ the BR reaches to the numerical values of the order of 10^{-2} for the small values of the radion mass, $m_r < 200\, GeV$. In the case of light flavor output

the addition of the new Higgs doublet and they enhance with the increasing values of the these couplings. Therefore, besides their important role in the construction of the FCNC in the tree level and the existence of the LFV interactions, these Yukawa couplings play a crucial role in the enhancement of the theoretical values of the BRs. In our calculations, we observe that the BRs of the processes we study are at most of the order of 10^{-8}, for the small values of radion mass m_r and for the large values of the Yukawa couplings, and, their sensitivities to m_r decrease with the increasing values of m_r. Among the LFV decays we study, the $r \to \tau^{\pm}\,\mu^{\pm}$ decay would be the most suitable one to measure its BR.

The paper is organized as follows: In Section 2, we present the effective vertex and the BRs of LFV r decays in the 2HDM, by respecting the RS1 scenario. Section 3 is devoted to a discussion and to our conclusions. In the appendix, we present the interaction vertices appearing in the calculations.

2 The LFV RS1 radion decay in the 2HDM

The RS1 model is an interesting candidate in order to explain the well known hierarchy problem. It is formulated as two 4D surfaces (branes) in 5D world in which the extra dimension is compactified into S^1/Z_2 orbifold. In this model, the SM fields are assumed to live on one of the brane, so called the TeV brane. On the other hand, the gravity peaks near the other brane, so called the Planck brane and extends into the bulk with varying strength. Here, 5D cosmological constant is non vanishing and both branes have equal and opposite tensions so that the low energy effective theory has flat 4D spacetime. The metric of such 5D world reads

$$ds^2 = e^{-2\,A(y)}\,\eta_{\mu\nu}\,dx^{\mu}\,dx^{\nu} - dy^2\,, \tag{1}$$

where $A(y) = k\,|y|$, k is the bulk curvature constant, y is the extra dimension parametrized as $y = R\,\theta$. The exponential factor $e^{-k\,L}$ with $L = R\,\pi$, is the warp factor which causes that all the mass terms are rescaled in the TeV brane. With a rough estimate $L \sim 30/k$, all mass terms are brought down to the TeV scale. The size L of extra dimension is related to the vacuum expectation of the field $L(x)$ and its fluctuation over the expectation value is called the radion field r. In order to avoid the violation of equivalence principle, $L(x)$ should acquire a mass and, to stabilize r, a mechanism was proposed by Goldberger and Wise [3], by introducing a potential for $L(x)$. Finally, the metric in 5D is defined as [4]

$$ds^2 = e^{-2\,A(y)-2\,F(x)}\,\eta_{\mu\nu}\,dx^{\mu}\,dx^{\nu} - (1+2\,F(x))\,dy^2\,, \tag{2}$$

$\mu\mu\,(ee)$ the numerical value of the BR is of the order of 10^{-4} (10^{-9}) for $m_r < 200\,GeV$ (see [9] for the explicit expressions of these decay widths).

where the radial fluctuations are carried by the scalar field $F(x)$,

$$F(x) = \frac{1}{\sqrt{6}\, M_{Pl}\, e^{-k\,L}}\, r(x)\,. \tag{3}$$

Here the field $r(x)$ is the normalized radion field (see [5]). At the orbifold point $\theta = \pi$ (TeV brane) the induced metric reads,

$$g^{ind}_{\mu\nu} = e^{-2\,A(L)-2\frac{\gamma}{v}\,r(x)}\,\eta_{\mu\nu}\,. \tag{4}$$

Here the parameter γ reads $\gamma = \frac{v}{\sqrt{6}\Lambda}$ with $\Lambda = M_{Pl}\, e^{-k\,L}$ and v is the vacuum expectation value of the SM Higgs boson. The radion is the additional degree of freedom of the 4D effective theory and we study the possible LFV decays of this field.

The FCNCs at tree level can exist in the 2HDM and they induce the flavor violating (FV) interactions with large BRs. The FV r decays, $r \to l_1^- l_2^+$, can exist at least in one loop level in the framework of the 2HDM. The part of action which carries the interaction, responsible for the LFV processes reads

$$\mathcal{S}_Y \;=\; \int d^4x \sqrt{-g^{ind}} \Big(\eta^E_{ij} \bar{l}_{iL} \phi_1 E_{jR} + \xi^E_{ij} \bar{l}_{iL} \phi_2 E_{jR} + h.c. \Big) \;, \tag{5}$$

where L and R denote chiral projections $L(R) = 1/2(1 \mp \gamma_5)$, ϕ_i for $i = 1, 2$, are two scalar doublets, l_{iL} (E_{jR}) are lepton doublets (singlets), ξ^{E}_{ij} [2] and η^E_{ij}, with family indices i, j , are the Yukawa couplings and ξ^E_{ij} induce the FV interactions in the leptonic sector. Here g^{ind} is the determinant of the induced metric on the TeV brane where the 2HDM particles live. Here, we assume that the Higgs doublet ϕ_1 has a non-zero vacuum expectation value to ensure the ordinary masses of the gauge fields and the fermions, however, the second doublet has no vacuum expectation value, namely, we choose the doublets ϕ_1 and ϕ_2 and their vacuum expectation values as

$$\phi_1 = \frac{1}{\sqrt{2}} \left[\left(\begin{array}{c} 0 \\ v + H^0 \end{array} \right) + \left(\begin{array}{c} \sqrt{2}\chi^+ \\ i\chi^0 \end{array} \right) \right] ; \phi_2 = \frac{1}{\sqrt{2}} \left(\begin{array}{c} \sqrt{2}H^+ \\ H_1 + iH_2 \end{array} \right) \;, \tag{6}$$

and

$$< \phi_1 > = \frac{1}{\sqrt{2}} \left(\begin{array}{c} 0 \\ v \end{array} \right) \; ; < \phi_2 > = 0\;. \tag{7}$$

This choice ensures that the mixing between neutral scalar Higgs bosons is switched off and it would be possible to separate the particle spectrum so that the SM particles are collected in the

[2] In the following, we replace ξ^E with ξ^E_N where "N" denotes the word "neutral".

first doublet and the new particles in the second one [3]. The action in eq. (5) is responsible for the tree level $S-l_1-l_2$ (l_1 and l_2 are different flavors of charged leptons, S denotes the neutral new Higgs boson, $S=h^0, A^0$) interaction (see Fig. 1-d, e) and the four point $r-S-l_1-l_2$ interaction (see Fig. 1-c) where r is the radion field. The latter interaction is coming from the determinant factor $\sqrt{-g^{ind}}=e^{-4\,A(L)-4\frac{\gamma}{v}\,r(x)}$. Notice that the term $e^{-4\,A(L)}$ in $\sqrt{-g^{ind}}$ is embedded into the redefinitions of the fields on the TeV brane, namely, they are warped as $S\rightarrow e^{A(L)}\,S_{warp}$, $l\rightarrow e^{3\,A(L)/2}\,l_{warp}$ and in the following we use warped fields without the *warp* index.

On the other hand, the part of new scalar action

$$\mathcal{S}_2 \;=\; \int d^4x\sqrt{-g^{ind}}\Big(g^{ind\,\mu\nu}\,(D_\mu\,\phi_2)^\dagger\,D_\nu\,\phi_2-m_S^2\,\phi_2^\dagger\,\phi_2\Big) \tag{8}$$

leads to

$$\mathcal{S'}_2=\frac{1}{2}\int d^4x\left\{e^{-2\frac{\gamma}{v}\,r}\eta^{\mu\nu}\left(\partial_\mu\,h^0\partial_\nu\,h^0+\partial_\mu\,A^0\partial_\nu\,A^0\right)-e^{-4\frac{\gamma}{v}\,r}\,(m_{h^0}^2\,h^0\,h^0+m_{A^0}^2\,A^0\,A^0)\right\}, \tag{9}$$

which carries the $S-S-r$ interaction[4] (see Fig. 1-b).

Finally, the interaction of leptons with the radion field is carried by the action (see [6])

$$\mathcal{S}_3 \;=\; \int d^4x\sqrt{-g^{ind}}\left(g^{ind\,\mu\nu}\,\bar{l}\,\gamma_\mu\,i\,D_\nu\,l-m_l\,\bar{l}\,l\right), \tag{11}$$

where

$$D_\mu\,l=\partial_\mu\,l+\frac{1}{2}\,w_\mu^{ab}\,\Sigma_{ab}\,l\,, \tag{12}$$

with $\Sigma_{ab}=\frac{1}{4}[\gamma_a,\gamma_b]$. Here w_μ^{ab} is the spin connection and, by using the vierbein fields e_μ^a, it can be calculated (linear in r) as

$$w_\mu^{ab}=-\frac{\gamma}{v}\partial_\nu\,r\,(e^{\nu b}\,e_\mu^a-e^{\nu a}\,e_\mu^b)\,. \tag{13}$$

[3] Here H_1 (H_2) is the well known mass eigenstate h^0 (A^0).

[4] In general, there is no symmetry which forbids the curvature-scalar interaction,

$$\mathcal{S}_\xi=\int d^4x\,\sqrt{-g^{ind}}\,\xi\,\mathcal{R}\,H^\dagger\,H\,, \tag{10}$$

where ξ is a restricted positive parameter and H is the Higgs scalar field [5, 13, 14]. This interaction results in the radion-(SM or new) Higgs mixing which can bring a sizeable contribution to the physical quantities studied. Here, we assume that there is no mixing between first and second doublet and only the first Higgs doublet has vacuum expectation value. Therefore, we choose that there exists a mixing between the radion and the SM Higgs field, but not between the radion and the new Higgs fields. This is the case that the lepton flavor violation is not affected by the mixing since the SM Higgs field is not responsible for the FCNC current at tree level.

Notice that the vierbein fields are the square root of the metric and they satisfy the relation

$$e^{\mu}_{a}\, e^{a\nu} = g^{ind\ \mu\nu}\,. \tag{14}$$

Using eqs. (11)-(14), one gets the part of the action which describes the tree level $l-l-r$ interaction (see Fig.1-a) as

$$\mathcal{S}'_3 \;=\; \int d^4x \left\{ -3\frac{\gamma}{v}\, r\,\bar{l}\, i\,\partial\!\!\!/ l - 3\frac{\gamma}{2\,v}\,\bar{l}\, i\,\partial\!\!\!/ r\, l + 4\,\frac{\gamma}{v}\, m_l\, r\,\bar{l}\, l \right\}. \tag{15}$$

At this stage, we would like to discuss briefly the case that the gauge fields and the leptons are also accessible to the extra dimension. With the addition of Dirac mass term $m_D(y) = m\frac{A'(y)}{k}$ ($A'(y) = \frac{dA(y)}{dy}$) to the lagrangian of bulk fermions, the fermion mass hierarchy can be obtained since they have different locations, regulated by a localization parameter $c = m/k$, in the extra dimension (see for example [16, 17, 18, 19]). Furthermore, the SM fermions are obtained by considering $SU(2)_L$ doublet ψ_L and singlet ψ_R with separate Z_2 projection conditions: $Z_2\psi_R = \gamma_5\psi_R$ and $Z_2\psi_L = -\gamma_5\psi_L$ (see for example [20]) and the localization parameters c_L and c_R assigned to each left and right handed fermion. If $c_{L;R} > \frac{1}{2}$ ($c_{L;R} < \frac{1}{2}$), the zero mode left;right handed fermions are localized near the hidden (visible) brane and, for $c_{L;R} = \frac{1}{2}$, they have constant profiles. Notice that the parameters c_L and c_R should be restricted such that the observed masses of fermions are obtained. In addition to the SM fermions (the zero mode ones) the KK modes of left and right handed fermions arise and these modes depend on the localization parameters c_L and c_R. In this scenario, the BRs of the LFV radion decays become sensitive to the different locations of left and right handed (zero mode and KK mode) leptons. This sensitivity is due to the couplings coming from $r - l^{(n)}_{iL(R)} - l^{(n)}_{iR(L)}$, $r - l^{(n)}_{iL(R)} - l^{(n)}_{iL(R)}$ and $S - l^{(n)}_{iL(R)} - l^{(n)}_{iR(L)}$ interactions, where $S = h^0, A^0$ and $n = 0, 1, 2, ...$ Here we can take two different possibilities: The first possibility is that the existence of the LFV is based on the different locations of different flavors (see for example [21, 22, 23]). In this case the new Yukawa couplings, appearing with the interaction of zero mode leptons and new Higgs bosons, sensitive to the locations of the corresponding leptons and the sources of the flavor violation are explicitly the localization parameters. If the leptons are far from (near to) the visible brane the couplings are suppressed (enhanced). Furthermore, the strengths of the couplings of KK mode leptons and new Higgs bosons are regulated by the locations of the lepton fields. In the second possibility, the flavor violation is carried by the new Yukawa couplings in four dimensions by assuming that the localization effects are embedded into the definition of new Yukawa couplings and, with the additional effects coming from the KK mode leptons, the role of extra dimension becomes the enhancement in the physical quantities . In both scenarios, the couplings of the radion with the leptons are regulated by the localization of the zero mode leptons and there exists an additional effect coming from the radion-KK mode lepton vertices. At first sight, it is expected that if the zero leptons are far from (near to) the visible brane these couplings are suppressed (enhanced). However, one needs a detailed analysis to take into account the bulk lepton contributions and their localization effects.

Now, we are ready to calculate the matrix element for the LFV radion decay. The decay of the radion to leptons with different flavors exits at least in one loop order, with the help of internal new Higgs bosons $S = h^0, A^0$. The possible vertex and self energy diagrams are presented in Fig. 2. After addition of all these diagrams, the divergences which occur in the loop integrals are eliminated and the matrix element square for this decay is obtained as

$$|M|^2 = 2\Big(m_r^2 - (m_{l_1^-} + m_{l_2^+})^2\Big)\, |A|^2 \,, \tag{16}$$

where

$$A = f^{self}_{h^0} + f^{self}_{A^0} + f^{vert}_{h^0} + f^{vert}_{A^0} + f^{vert}_{h^0 h^0} + f^{vert}_{A^0 A^0} \,, \tag{17}$$

and the explicit expressions of the functions appearing in eq. (17) are given in Appendix B. Notice that in eq. (23) the flavor changing couplings $\xi^E_{N,l_j i}$ represent the effective interaction between the internal lepton i, $(i = e, \mu, \tau)$ and the outgoing $j = 1\,(j = 2)$ lepton (anti lepton). Here, we choose the couplings $\xi^E_{N,l_j i}$ real.

Finally, the BR for $r \to l_1^-\, l_2^+$ can be obtained by using the matrix element square as

$$BR(r \to l_1^-\, l_2^+) = \frac{1}{16\,\pi\, m_r}\, \frac{|M|^2}{\Gamma_r} \,, \tag{18}$$

where Γ_r is the total decay width of radion r. In our numerical analysis, we consider the BR due to the production of sum of charged states, namely

$$BR(r \to l_1^{\pm}\, l_2^{\pm}) = \frac{\Gamma(r \to (\bar{l}_1\, l_2 + \bar{l}_2\, l_1))}{\Gamma_r} \,. \tag{19}$$

3 Discussion

In four dimensions, the higher dimensional gravity is observed as it has new states with spin 2,1 and 0, so called, the graviton, the gravivector, the graviscalar. These states interact with the particles in the underlying theory. In the RS1 model with one extra dimension, the spin 0 gravity particle radion r interacts with the particles of the theory (2HDM in our case) on the

TeV brane and this interaction occurs over the trace of the energy-momentum tensor T^{μ}_{μ} with the strength $1/\Lambda_r$,

$$\mathcal{L}_{int} = \frac{r}{\Lambda_r} T^{\mu}_{\mu} \, , \qquad (20)$$

where Λ_r is at the order of TeV. The radion interacts with gluon (g) pair or photon (γ) pair in one loop order from the trace anomaly. For the radion mass $m_r \leq 150 \, GeV$, the decay width is dominated by $r \to gg$. For the masses which are beyond the WW and ZZ thresholds, the main decay mode is $r \to WW$. In the present work, we study the possible LFV decays of the RS1 radion in the 2HDM and estimate the BRs of these decays for different values of radion masses. We take the total decay width Γ_r of the radion by considering the dominant decays $r \to gg \, (\gamma\gamma, ff, W^+W^-, ZZ, SS)$ where S are the neutral Higgs particles (see [9] for the explicit expressions of these decay widths). Here, we include the possible processes in the Γ_r according to the mass of the radion.

The flavor violating r decays $r \to l_1^- l_2^+$ can exist at least in one loop level, in the framework of the 2HDM and the flavor violation is carried by the Yukawa couplings $\bar{\xi}^{E}_{N,ij}$[5]. In the version of 2HDM where the FCNC are permitted, these couplings are free parameters which should be restricted by using the present and forthcoming experiments. At first, we assume that these couplings are symmetric with respect to the flavor indices i and j. Furthermore, we take that the couplings which contain at least one τ index are dominant and we choose a broad range for these couplings, by respecting the upper limit prediction of $\bar{\xi}^{E}_{N,\tau\mu}$ (see [24] and references therein), which is obtained by using the experimental uncertainty, 10^{-9}, in the measurement of the muon anomalous magnetic moment and by assuming that the new physics effects can not exceed this uncertainty. For the coupling $\bar{\xi}^{E}_{N,\tau e}$, the restriction is estimated by using this upper limit and the experimental upper bound of BR of $\mu \to e\gamma$ decay, BR $\leq 1.2 \times 10^{-11}$ [25]. Finally, this coupling is taken in the range $10^{-3} - 10^{-1} \, GeV$ (see [26]). For the Yukawa coupling $\bar{\xi}^{E}_{N,\tau\tau}$, we have no explicit restriction region and we use the numerical values which are greater than $\bar{\xi}^{E}_{N,\tau\mu}$. Throughout our calculations we use the input values given in Table (1).

In Fig.3 we present m_r dependence of the BR ($r \to \tau^{\pm} \, \mu^{\pm}$). The solid-dashed lines represent the BR ($r \to \tau^{\pm} \, \mu^{\pm}$) for $\bar{\xi}^{E}_{N,\tau\tau} = 100 \, GeV$, $\bar{\xi}^{E}_{N,\tau\mu} = 10 \, GeV$- $\bar{\xi}^{E}_{N,\tau\tau} = 10 \, GeV$, $\bar{\xi}^{E}_{N,\tau\mu} = 1 \, GeV$. It is observed that the BR ($r \to \tau^{\pm} \, \mu^{\pm}$) is of the order of the magnitude of 10^{-8} for the large values of the couplings and the radion mass values $\sim 200 \, GeV$. For the heavy masses of the radion the BR is stabilized to the values of the order of 10^{-9}.

[5]The dimensionfull Yukawa couplings $\bar{\xi}^{E}_{N,ij}$ are defined as $\xi^{E}_{N,ij} = \sqrt{\frac{4 \, G_F}{\sqrt{2}}} \, \bar{\xi}^{E}_{N,ij}$.

Parameter	Value
m_μ	0.106 (GeV)
m_τ	1.78 (GeV)
m_{h^0}	100 (GeV)
m_{A^0}	200 (GeV)
G_F	$1.1663710^{-5} (GeV^{-2})$

Table 1: The values of the input parameters used in the numerical calculations.

Fig.4 is devoted to m_r dependence of the BR ($r \rightarrow \tau^\pm\, e^\pm$) and BR ($r \rightarrow \mu^\pm\, e^\pm$). The solid-dashed lines represent the BR ($r \rightarrow \tau^\pm\, e^\pm$) for $\bar{\xi}^E_{N,\tau\tau} = 100\, GeV$, $\bar{\xi}^E_{N,\tau e} = 0.1\, GeV$- $\bar{\xi}^E_{N,\tau\tau} = 10\, GeV$, $\bar{\xi}^E_{N,\tau e} = 0.1\, GeV$. The small dashed line represents the BR ($r \rightarrow \mu^\pm\, e^\pm$) for $\bar{\xi}^E_{N,\tau\mu} = 1\, GeV$, $\bar{\xi}^E_{N,\tau e} = 0.1\, GeV$. This figure shows that the BR ($r \rightarrow \tau^\pm\, \mu^\pm$) is of the order of the magnitude of 10^{-12} for the large values of the couplings and the radion mass values $\sim 200\, GeV$. For the heavy masses of the radion, this BR reaches to the values less than 10^{-14}. The BR ($r \rightarrow \mu^\pm\, e^\pm$) is of the order of 10^{-15} for $m_r \sim 200\, GeV$ and for the intermediate values of Yukawa couplings. These BRs, especially BR ($r \rightarrow \mu^\pm\, e^\pm$), are negligibly small.

Now, we present the Yukawa coupling dependencies of the BRs of the decays under consideration, for different radion masses .

Fig.5 represents the $\bar{\xi}^E_{N,\tau\tau}$ dependence of the BR ($r \rightarrow \tau^\pm\, \mu^\pm$) for $\bar{\xi}^E_{N,\tau\mu} = 10\, GeV$. The solid-dashed-small dashed lines represent the BR for the radion masses $m_r = 200 - 500 - 1000\, GeV$. This figure shows that the BR is sensitive to the radion mass and, obviously, it is enhanced two orders of magnitude in the range $10\, GeV \leq \bar{\xi}^E_{N,\tau\tau} \leq 100\, GeV$.

In Fig.6, we present the $\bar{\xi}^E_{N,\tau\tau}$ dependence of the BR ($r \rightarrow \tau^\pm\, e^\pm$) for $\bar{\xi}^E_{N,\tau e} = 0.1\, GeV$. The solid-dashed-small dashed lines represent the BR for the radion masses $m_r = 200 - 500 - 1000\, GeV$. Similar to the $r \rightarrow \tau^\pm\, \mu^\pm$ decay, the BR is strongly sensitive to the radion mass.

4 Conclusion

The LFV decays of the radion in the RS1 model strongly depend on the radion mass and the Yukawa couplings. The BR for $r \rightarrow \tau^\pm\, \mu^\pm$ decay is of the order of 10^{-8} for the small values of radion mass m_r and it decreases with the increasing values of m_r. On the other hand, the BRs for $r \rightarrow \tau^\pm\, e^\pm$ ($r \rightarrow \mu^\pm\, e^\pm$) decays are of the order of 10^{-12} (10^{-15}) for the small values of m_r. These results show that, among these processes, the LFV $r \rightarrow \tau^\pm\, \mu^\pm$ decay would be the most appropriate one to measure its BR. The most probable production of radion is due to the gluon fusion, $gg \rightarrow r$ [9]) and, based on the existing cross section values for the radion production via gluon fusion and the typical integrated luminosities expected at LHC, a rough estimation of the number of events for the $\tau^{\pm}\,\mu^{\pm}$ final state is missing at present. The goal being to check that this number of events is significant statistically, and hopefully, the forthcoming experimental results of this decay would be useful in order to test the possible signals coming from the extra dimensions and new physics which results in flavor violation.

A The vertices appearing in the present work

In this section we present the vertices appearing in our calculations. Here S denotes the new neutral Higgs bosons h^0 and A^0.

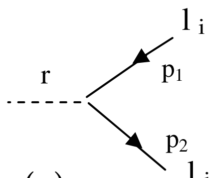

(a)

$$\frac{-i\gamma}{v}\left[\frac{3}{2}\,(\not{p}_1+\not{p}_2)-4\,m_{l_i}\right]$$

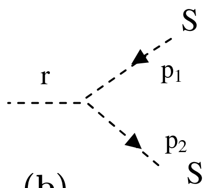

(b)

$$\frac{-2\,i\,\gamma}{v}\,(p_1.p_2-m_S^2)$$

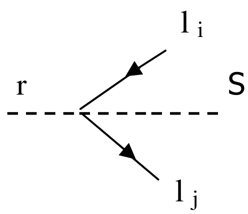

$$(S=h^0)\quad \frac{4\,i\gamma}{2\sqrt{2}\,v}\left[(\xi^E_{ij}+\xi^{E*}_{ji})+(\xi^E_{ij}-\xi^{E*}_{ji})\gamma_5\right]$$

$$(S=A^0)\quad \frac{-4\,\gamma}{2\sqrt{2}\,v}\left[(\xi^E_{ij}-\xi^{E*}_{ji})+(\xi^E_{ij}+\xi^{E*}_{ji})\gamma_5\right]$$

(c)

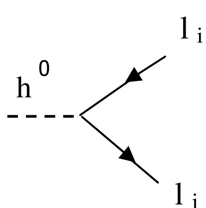

$$\frac{-i}{2\sqrt{2}}\left[(\xi^E_{ij}+\xi^{E*}_{ji})+(\xi^E_{ij}-\xi^{E*}_{ji})\gamma_5\right]$$

(d)

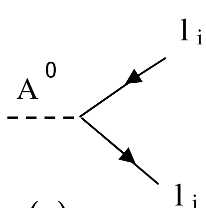

$$\frac{1}{2\sqrt{2}}\left[(\xi^E_{ij}-\xi^{E*}_{ji})+(\xi^E_{ij}+\xi^{E*}_{ji})\gamma_5\right]$$

(e)

Figure 1: The vertices used in the present work.

B The explicit expressions appearing in the text

The explicit expressions of functions $f^{self}_{h^0\,(A^0)}$, $f^{ver}_{h^0\,(A^0)}$, $f^{ver}_{h^0\,h^0}$ and $f^{ver}_{A^0\,A^0}$ in eq.(17) are given by

$$\begin{aligned}
f^{self}_{h^0} &= \frac{\gamma}{128\,v\,\pi^2\,(w'_h-w_h)}\int_0^1 dx\, m_{h^0}\Bigg\{\Big(\eta^V_i\,(x-1)\,w_h-\eta^+_i\,z_{ih}\Big)\Big(3\,w'_h-5\,w_h\Big)\,ln\,\frac{L^{self}_{1,h^0}\,m^2_{h^0}}{\mu^2}\\
&+ \Big(\eta^V_i\,(x-1)\,w'_h-\eta^+_i\,z_{ih}\Big)\Big(5\,w'_h-3\,w_h\Big)\,ln\,\frac{L^{self}_{2,h^0}\,m^2_{h^0}}{\mu^2}\Bigg\}\,,\\
f^{self}_{A^0} &= \frac{\gamma}{128\,v\,\pi^2\,(w'_A-w_A)}\int_0^1 dx\;,m_{A^0}\Bigg\{\Big(\eta^V_i\,(x-1)\,w_A+\eta^+_i\,z_{iA}\Big)\Big(3\,w'_A-5\,w_A\Big)\,ln\,\frac{L^{self}_{1,A^0}\,m^2_{A^0}}{\mu^2}\\
&+ \Big(\eta^V_i\,(x-1)\,w'_A+\eta^+_i\,z_{iA}\Big)\Big(5\,w'_A-3\,w_A\Big)\,ln\,\frac{L^{self}_{2,A^0}\,m^2_{A^0}}{\mu^2}\Bigg\}\,,\\
f^{vert}_{h^0} &= \frac{\gamma}{128\,v\,\pi^2}\int_0^1 dx\int_0^{1-x} dy\Bigg\{\frac{m_{h^0}}{L^{ver}_{h^0}}\Bigg[\eta^V_i\Bigg(3\,z^2_{rh}\Big(y\,(1-y)\,w'_h+x^2\,(4\,y-1)\,w_h\\
&+ x\,((1-3\,y)\,w_h+y\,(4\,y-3)\,w'_h)\Big)+5\,z^2_i\Big((2\,y-1)\,w'_h+(2\,x-1)\,w_h\Big)\\
&- 3\,(x+y-1)\Big(x\,(4\,x-3)\,w^3_h+y\,(4\,y-3)\,w'^3_h\Big)\\
&- 3\,w_h\,w'_h\,(x+y-1)\Big((1-y+x\,(4\,y-2))\,w_h+(1-2\,y+x\,(4\,y-1))\,w'_h\Big)\\
&+ 3\,(x+y-1)\Big((2\,x-1)\,w_h+(2\,y-1)\,w'_h\Big)\Bigg)\\
&+ \eta^+_i\,z_{ih}\Bigg((x+y-1)\Big(-4+2\,w'_h\,w_h+w'^2_h\,(8\,y-3)+w^2_h\,(8\,x-3)\Big)\\
&- \Big(8\,z^2_{ih}+z^2_{rh}\,((8\,y-3)\,x-3\,y)\Big)\Bigg)\Bigg]\\
&- m_{h^0}\,ln\,\frac{L^{ver}_{h^0}\,m^2_{h^0}}{\mu^2}\Bigg(9\,\eta^V_i\Big(w'_h\,(2\,y-1)+w_h\,(2\,x-1)\Big)-8\,\eta^+_i\,z_{ih}\Bigg)\Bigg\}\,,\\
f^{vert}_{A^0} &= \frac{\gamma}{128\,v\,\pi^2}\int_0^1 dx\int_0^{1-x} dy\Bigg\{\frac{m_{A^0}}{L^{ver}_{A^0}}\Bigg[\eta^V_i\Bigg(3\,z^2_{rA}\Big(y\,(1-y)\,w'_A+x^2\,(4\,y-1)\,w_A\\
&+ x\,((1-3\,y)\,w_A+y\,(4\,y-3)\,w'_A)\Big)+5\,z^2_i\Big((2\,y-1)\,w'_A+(2\,x-1)\,w_A\Big)\\
&- 3\,(x+y-1)\Big(x\,(4\,x-3)\,w^3_A+y\,(4\,y-3)\,w'^3_A\Big)\\
&- 3\,w_A\,w'_A\,(x+y-1)\Big((1-y+x\,(4\,y-2))\,w_A+(1-2\,y+x\,(4\,y-1))\,w'_A\Big)\\
&+ 3\,(x+y-1)\Big((2\,x-1)\,w_A+(2\,y-1)\,w'_A\Big)\Bigg)\\
&+ \eta^+_i\,z_{iA}\Bigg((x+y-1)\Big(-4+2\,w'_A\,w_A+w'^2_A\,(8\,y-3)+w^2_A\,(8\,x-3)\Big)\\
&- \Big(8\,z^2_{iA}+z^2_{rA}\,((8\,y-3)\,x-3\,y)\Big)\Bigg)\Bigg]\\
&- m_{A^0}\,ln\,\frac{L^{ver}_{A^0}\,m^2_{A^0}}{\mu^2}\Bigg(9\,\eta^V_i\Big(w'_A\,(2\,y-1)+w_A\,(2\,x-1)\Big)+8\,\eta^+_i\,z_{iA}\Bigg)\Bigg\}\,,
\end{aligned}$$

$$
\begin{aligned}
f^{vert}_{h^0\,h^0} &= \frac{\gamma}{64\,v\,\pi^2}\int_0^1 dx\int_0^{1-x} dy\left\{\frac{m_{h^0}}{L^{ver}_{h^0\,h^0}}\left[\eta_i^V\left(z_{rh}^2\left(y-1+x\,(1-4\,y)\right)(x\,w_h+y\,w'_h)\right.\right.\right.\\
&+ y\,(x+y-1)\,w'_h\left((4\,x-1)\,w_h^2+(4\,y-1)\,w_h'^2\right)\\
&+ \left.w_h^3\,x\,(x+y-1)\,(4\,x-1)+(x+y-1)\left(2\,y\,w'_h+x\,w_h\,(2+w_h'^2\,(4\,y-1))\right)\right)\\
&+ \left.\eta_i^+\left((x+y-1)\,z_{ih}\left((4\,y-1)\,w_h'^2+(4\,x-1)\,w_h^2+2\right)-z_{ih}\,z_{rh}^2\left((4\,y-1)\,x-y+1\right)\right)\right]\\
&- \left.m_{h^0}\,ln\,\frac{L^{ver}_{h^0\,h^0}\,m^2_{h^0}}{\mu^2}\left(\eta_i^V\left(w'_h\,(1-6\,y)+w_h\,(1-6\,x)\right)-4\,\eta_i^+\,z_{ih}\right)\right\},\\
f^{vert}_{A^0\,A^0} &= \frac{\gamma}{64\,v\,\pi^2}\int_0^1 dx\int_0^{1-x} dy\left\{\frac{m_{A^0}}{L^{ver}_{A^0\,A^0}}\left[\eta_i^V\left(z_{rA}^2\left(y-1+x\,(1-4\,y)\right)(x\,w_A+y\,w'_A)\right.\right.\right.\\
&+ y\,(x+y-1)\,w'_A\left((4\,x-1)\,w_A^2+(4\,y-1)\,w_A'^2\right)\\
&+ \left.w_A^3\,x\,(x+y-1)\,(4\,x-1)+(x+y-1)\left(2\,y\,w'_A+x\,w_A\,(2+w_A'^2\,(4\,y-1))\right)\right)\\
&+ \left.\eta_i^+\left((x+y-1)\,z_{iA}\left((4\,y-1)\,w_A'^2+(4\,x-1)\,w_A^2+2\right)-z_{iA}\,z_{rA}^2\left((4\,y-1)\,x-y+1\right)\right)\right]\\
&- \left.m_{A^0}\,ln\,\frac{L^{ver}_{A^0\,A^0}\,m^2_{A^0}}{\mu^2}\left(\eta_i^V\left(w'_A\,(1-6\,y)+w_A\,(1-6\,x)\right)+4\,\eta_i^+\,z_{iA}\right)\right\}, \qquad (21)
\end{aligned}
$$

where

$$
\begin{aligned}
L^{self}_{1,h^0(A^0)} &= 1+x^2\,w^2_{h(A)}+x\,(z^2_{ih(iA)}-w^2_{h(A)}-1)\,,\\
L^{self}_{2,h^0(A^0)} &= 1+x^2\,w'^2_{h(A)}+x\,(z^2_{ih(iA)}-w'^2_{h(A)}-1)\,,\\
L^{ver}_{h^0(A^0)} &= x^2\,w^2_{h(A)}+(y-1)\,(w'^2_{h(A)}\,y-1)+x\,(y\,w'^2_{h(A)}+(y-1)\,w^2_{h(A)}-y\,z^2_{rh(rA)}-1)\,,\\
L^{ver}_{h^0\,h^0(A^0\,A^0)} &= x^2\,w^2_{h(A)}+(1+w'^2_{h(A)}\,(y-1))\,y+x\,(1+w^2_{h(A)}\,(y-1)+w'^2_{h(A)}\,y-z^2_{rh(rA)}\,y)\,,
\end{aligned}
\qquad (22)
$$

with the parameters $w_{h(A)}=\frac{m_{l_1^-}}{m_{h^0(A^0)}}$, $w'_{h(A)}=\frac{m_{l_2^+}}{m_{h^0(A^0)}}$, $z_{rh(rA)}=\frac{m_r}{m_{h^0(A^0)}}$, $z_{ih(iA)}=\frac{m_i}{m_{h^0(A^0)}}$ and

$$
\begin{aligned}
\eta_i^V &= \xi^E_{N,l_1 i}\xi^{E\,*}_{N,i l_2}+\xi^{E\,*}_{N,i l_1}\xi^E_{N,l_2 i}\,,\\
\eta_i^+ &= \xi^{E\,*}_{N,i l_1}\xi^{E\,*}_{N,i l_2}+\xi^E_{N,l_1 i}\xi^E_{N,l_2 i}\,.
\end{aligned}
\qquad (23)
$$

References

[1] N. Arkani-Hamed, S. Dimopoulos and G. Dvali, *Phys. Lett.* **B429** (1998) 263; I. Antoniadis, *et al.*, *Phys. Lett.* **B436** (1998) 257; I. Antoniadis, S. Dimopoulos, G. Dvali, Nucl. Phys. **B516** (1998) 70.

[2] L. Randall, R.Sundrum, *Phys. Rev. Lett.* **83** (1999) 3370; L. Randall, R.Sundrum, *Phys. Rev. Lett.* **83** (1999) 4690;

[3] W. D. Goldberger, M. B. Wise, *Phys. Rev. Lett.* **D 83** (1999) 4922.

[4] C. Charmousis, R. Gregory, V. A. Rubakov, *Phys. Rev.* **D 62** (2000) 067505.

[5] C. Csaki, M. L. Graesser, G. D. Gribs, *Phys. Rev.* **D 63** (2001) 065002.

[6] P. K. Das, hep-ph 0407041; P. K. Das, *Phys. Rev.* **D 72** (2005) 055009

[7] G. D. Kribs, eConf C010630 (2001) P317, hep-ph/0110242

[8] T. Han, G. D. Kribs, B. McElrath *Phys. Rev.* **D 64** (2001) 076003.

[9] K. Cheung, *Phys. Rev.* **D 63** (2001) 056007.

[10] K. Cheung, hep-ph/0408200.

[11] G. F. Giudice, R. Rattazzi, J. D. Wells, *Nucl. Phys.* **B 595** (2001) 250.

[12] U. Mahanta, A. Datta *Phys. Lett.* **B 483** (2000) 196.

[13] K. Cheung, C. S. Kim, J. Song, *Phys. Rev.* **D67**, 075017, (2003).

[14] C. Csaki, hep-ph/0404096.

[15] B. Pontecorvo, *Zh. Eksp. Teor. Fiz.* **33** (1957) 549, Z. Maki, M. Nakagawa, and S. Sakata, *Prog. Theor. Phys.* **28** (1962) 870, B. Pontecorvo, *Sov. Phys. JETP* **26** (1968) 984.

[16] T. Gherghetta, A. Pomarol, *Nucl. Phys.* **B586** 141, (2000).

[17] Y. Grossman, M. Neubert, *Phys. Lett.* **B474** 361, (2000).

[18] S. J. Huber, hep-ph/0211056, (2002).

[19] S. J. Huber, *Nucl. Phys.* **B666** 269, (2003).

[20] S. Chang, J. Hisano, H. Nakano, N. Okada, M. Yamaguchi, *Phys. Rev.* **D62** 084025, (2000).

[21] K. Agashe, G. Perez and A. Soni, *Phys. Rev.* **D71** 016002, (2005).

[22] K.Agashe, A. E. Blechman and F. Petriello, *Phys. Rev.* **D74** 053011, (2006).

[23] F. Ledroit, G. Moreau, J. Morel, *JHEP* **09** 071, (2007).

[24] E. Iltan, H. Sundu, *Acta Phys.Slov.* **53** 17, (2003).

[25] M. L. Brooks et. al., MEGA Collaboration, *Phys. Rev. Lett.* **83**, 1521 (1999).

[26] E. Iltan, *Phys. Rev.* **D64**, 115005, (2001); *Phys. Rev.* **D64** 013013, (2001).

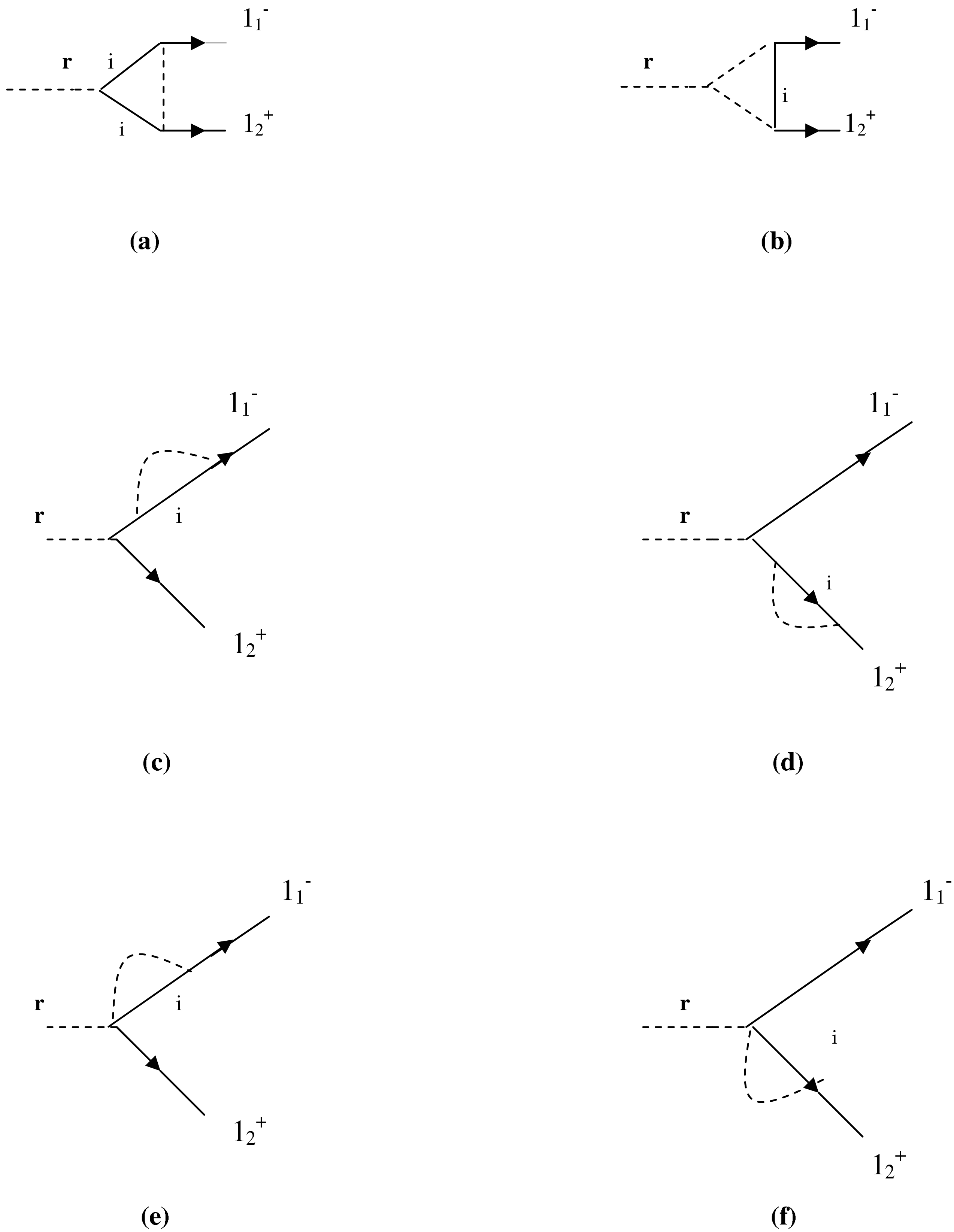

Figure 2: One loop diagrams contribute to $r \rightarrow l_1^- \, l_2^+$ decay due to the neutral Higgs bosons h_0 and A_0 in the 2HDM. i represents the internal lepton, l_1^- (l_2^+) outgoing lepton (anti lepton), internal dashed line the h_0 and A_0 fields.

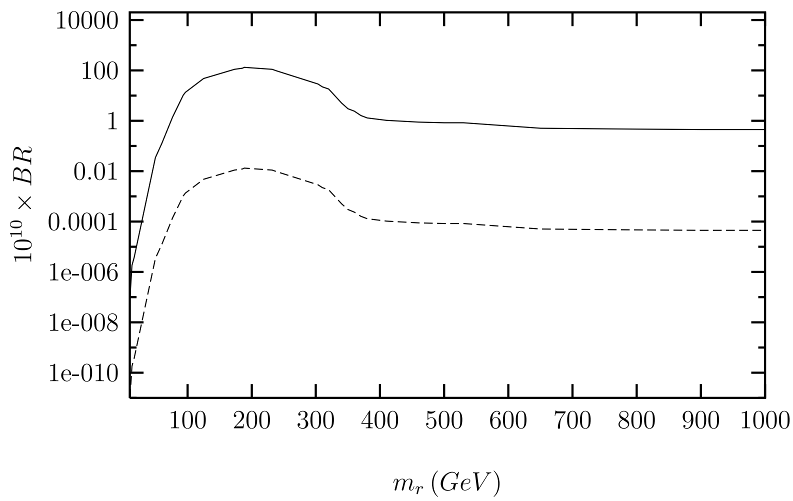

Figure 3: m_r dependence of the BR ($r \to \tau^{\pm}\,\mu^{\pm}$). The solid-dashed lines represent the BR($r \to \tau^{\pm}\,\mu^{\pm}$) for $\bar{\xi}^{E}_{N,\tau\tau} = 100\,GeV$, $\bar{\xi}^{E}_{N,\tau\mu} = 10\,GeV$- $\bar{\xi}^{E}_{N,\tau\tau} = 10\,GeV$, $\bar{\xi}^{E}_{N,\tau\mu} = 1\,GeV$.

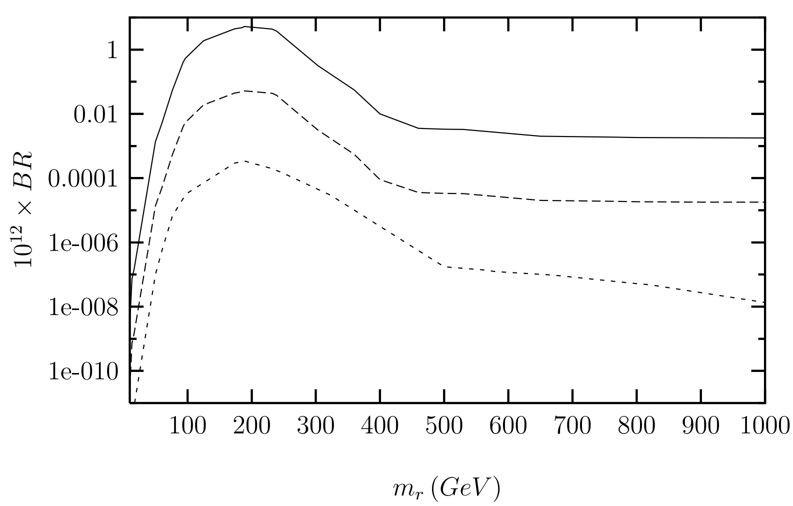

Figure 4: m_r dependence of the BR ($r \to l_1^{\pm}\,l_2^{\pm}$). The solid-dashed lines represent the BR($r \to \tau^{\pm}\,e^{\pm}$) for $\bar{\xi}^{E}_{N,\tau\tau} = 100\,GeV$, $\bar{\xi}^{E}_{N,\tau e} = 0.1\,GeV$- $\bar{\xi}^{E}_{N,\tau\tau} = 10\,GeV$, $\bar{\xi}^{E}_{N,\tau e} = 0.1\,GeV$. The small dashed line represents the BR ($r \to \mu^{\pm}\,e^{\pm}$) for $\bar{\xi}^{E}_{N,\tau\mu} = 1\,GeV$, $\bar{\xi}^{E}_{N,\tau e} = 0.1\,GeV$.

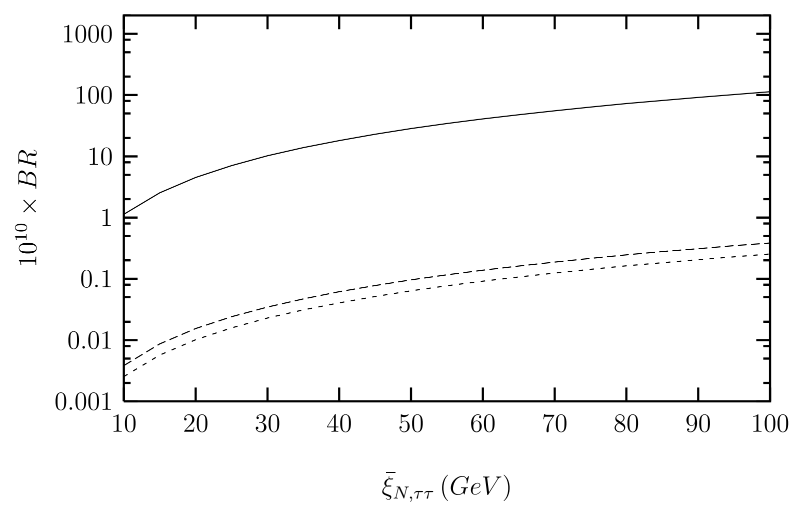

Figure 5: $\bar{\xi}^{E}_{N,\tau\tau}$ dependence of the BR($r \to \tau^{\pm}\,\mu^{\pm}$) for $\bar{\xi}^{E}_{N,\tau\mu} = 10\,GeV$. The solid-dashed-small dashed lines represent the BR for the radion masses $m_r = 200 - 500 - 1000\,GeV$.

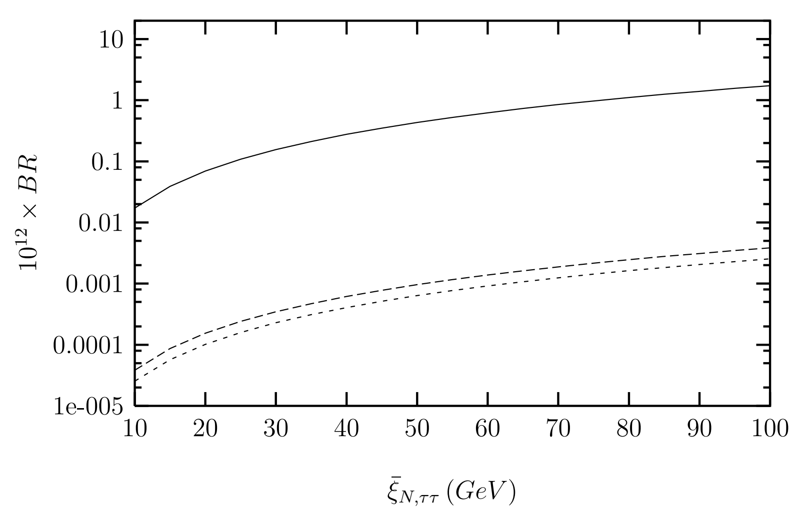

Figure 6: $\bar{\xi}^{E}_{N,\tau\tau}$ dependence of the BR($r \to \tau^{\pm}\,e^{\pm}$) for $\bar{\xi}^{E}_{N,\tau e} = 0.1\,GeV$. The solid-dashed-small dashed lines represent the BR for the radion masses $m_r = 200 - 500 - 1000\,GeV$.